Available online at www.sciencedirect.com
ScienceDirect
Bioorganic Chemistry 34 (2006) 325–336
BIOORGANIC CHEMISTRY
www.elsevier.com/locate/bioorg

Determinants of substrate specificity in KdcA, a thiamin diphosphate-dependent decarboxylase

Alejandra Yep, George L. Kenyon, Michael J. McLeish *

College of Pharmacy, University of Michigan, 428 Church Street, Ann Arbor, MI 48109-1065, USA

Received 28 July 2006
Available online 9 October 2006

Abstract

Thiamin diphosphate-dependent decarboxylases catalyze the non-oxidative decarboxylation of 2-keto carboxylic acids. Although they display relatively low sequence similarity, and broadly different range of substrates, these enzymes show a common homotetrameric structure. Here we describe a kinetic characterization of the substrate spectrum of a recently identified member of this class, the branched chain 2-keto acid decarboxylase (KdcA) from *Lactococcus lactis*. In order to understand the structural basis for KdcA substrate recognition we developed a homology model of its structure. Ser286, Phe381, Val461 and Met358 were identified as residues that appeared to shape the substrate binding pocket. Subsequently, site-directed mutagenesis was carried out on these residues with a view to converting KdcA into a pyruvate decarboxylase. The results show that the mutations all lowered the K_m value for pyruvate and both the S286Y and F381W variants also had greatly increased values of k_{cat} with pyruvate as a substrate.

Keywords: Benzoylformate; Phenylpyruvate; Pyruvate; 2-Keto acid; Mutagenesis; Homology model

1. Introduction

Pyruvate decarboxylase from *Zymomonas mobilis* (*Zm*PDC) and *Saccharomyces cerevisiae* (*Sc*PDC), benzoylformate decarboxylase from *Pseudomonas putida* (BFD) and

* Corresponding author. Fax: +1 734 615 3079.
E-mail address: mcleish@umich.edu (M.J. McLeish).

0045-2068/$ - see front matter © 2006 Elsevier Inc. All rights reserved.
doi:10.1016/j.bioorg.2006.08.005

indolepyruvate decarboxylase from *Enterobacter cloacae* (IPDC) all belong to a group of enzymes whose main function is the non-oxidative decarboxylation of 2-keto acids [1]. The X-ray structures of these enzymes, which utilize Mg^{2+} and thiamin diphosphate (ThDP) as cofactor, show that they are structurally similar [2–5]. However, while the PDCs prefer pyruvate as a substrate and, to a lesser extent, other aliphatic 2-keto acids [6], BFD prefers aromatic 2-keto acids [7] as does IPDC [8].

One of the intriguing features of these enzymes is that, with the exception of residues involved in binding ThDP, there is little strict conservation of other active site residues, at least in terms of sequence identity [4,8,9]. This is somewhat surprising as the differences between the natural substrates are mostly steric in nature (Fig. 1). However, there does appear to be some positional conservation of residues. This suggests that the active site architecture, as well as the chemistry of the cofactor and reaction intermediates, have played a dominant role in the evolution of enzymes of this type [4]. In our efforts towards understanding the evolution of substrate specificity in ThDP-dependent enzymes, site-directed mutagenesis was employed in an attempt to interconvert *Zm*PDC and BFD [10]. Although the interconversion was not particularly successful, a single mutation in either enzyme was able to bring about significantly enhanced decarboxylase activity with long (C5/C6) chain aliphatic keto acids. In fact, the I472A variant of *Zm*PDC was able to decarboxylate 2-ketohexanoic acid with a higher k_{cat}/K_m value than that of the WT enzyme with its natural substrate. Further, both this *Zm*PDC variant and the analogous A460I variant of BFD were able to decarboxylate branched chain keto acids with k_{cat}/K_m values greater than those of the WT enzymes [10].

Recently, the cloning of KdcA, a branched chain 2-keto acid decarboxylase, was reported [11]. The enzyme appeared to be involved in flavor formation in cheeses brought about by the actions of *Lactococcus lactis*, with 3-methyl-2-oxobutanoic acid being the preferred substrate (Scheme 1). Here we describe the overexpression of KdcA in *Escherichia coli* and a kinetic analysis of its substrate specificity. In addition, based on a homology model of

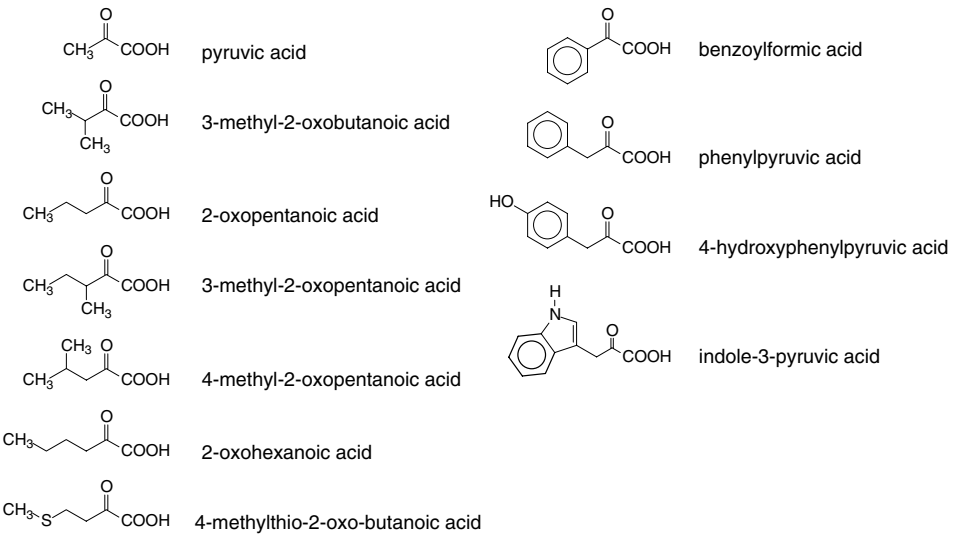

Fig. 1. Structures of substrates for the various 2-keto acid decarboxylases.

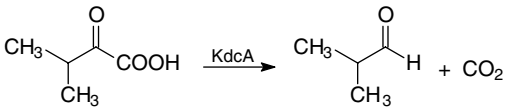

Scheme 1.

KdcA we have carried out a mutagenic analysis of several residues potentially involved in substrate binding.

2. Materials and methods

The plasmid pNZ500 [11], containing the *kdcA* gene was obtained from Nizo Food Research. Thiamin diphosphate and the various 2-keto acids were purchased from Sigma–Aldrich. Buffer salts were purchased from Fisher. All other reagents were of the highest purity available.

2.1. Homology modeling of KdcA

The three-dimensional structure of KdcA was modeled with Modeller 8v1 [12] using the crystal structures of *Zm*PDC (PDB code 1ZPD), *Sc*PDC complexed with pyruvamide (PDB code 1QPB), and IPDC (PDB code 1OVM), as templates. The initial multiple alignment was performed with ClustalW [13] and manually refined to include functionally conserved residues, predicted secondary structures, and hydrophobicity profiles. Secondary structures were predicted using the PSI-PRED program [14]. Different models of the monomer were generated and assessed by the VERIFY_3D [15] and PROCHECK programs [16], and the best model was chosen to model the dimeric and tetrameric forms of the enzyme. Figures were created with PyMOL (DeLano Scientific, http://pymol.sourceforge.net/), SwissPDBViewer ([17] www.expasy.org/spdbv/) and Pov-Ray (Persistence of Vision Raytracer Pty. Ltd., http://povray.org/). The PDB file for the model of the KdcA dimer is available as Supplementary material.

2.2. Amplification and site-directed mutagenesis of kdcA

The coding region of *kdcA* was amplified by PCR from plasmid pNZ500 [11] using the primers 5′-GGAGGAATGaCATGtATACAGTAGGAGATTGGAGATT-3′ and 5′-CATCATCCGTTGATATCTcgagATTTTGCTCA-3′. These primers contained changes from wild-type, denoted by lowercase letters, which introduced *Bsp*LU11I and *Xho*I restriction sites, respectively. The amplified fragment was gel purified, digested and subcloned into pET-24d (Novagen) previously digested with *Nco*I and *Xho*I. This construction added a 6× His tag to the C-terminus of the enzyme. The fidelity of the amplification was confirmed by sequencing the resulting plasmid, pET24d-KdcA-His, at the University of Michigan core facility.

Site-directed mutagenesis was performed using the QuikChange protocol and *Pfu* polymerase (Stratagene) using pET24d-KdcA-His as a template. The forward primers used for the mutagenesis are shown below, with the mutated codons underlined and, again, lowercase letters indicating base changes from the wild-type gene:

V461I: 5′-CATAAATAATGATGGTTATACAaTTGAAAGAGAAATCCAtGGAC CTACTC-3′
S286Y: 5′-GCTTGGAGTGAAGtTaACGGACTaCTCAACAGGTGCATTC-3′
F381W: 5′-GCTGAACAAGGAACCTCATggTTTGGAGCgTCAACAATTTTC-3′
M538W: 5′-GCGCCAAAATTACTGAAAAAAtgGGGTAAgcTtTTTGCTGAGC-3′.

In all primers additional silent mutations were introduced, generating new restriction sites for *Nco*I, *Hin*cII, *Hin*dIII and *Hin*cII, respectively. These were used for the initial screening for mutants by restriction analysis. The coding regions of the resulting plasmids were sequenced to ensure that only the intended mutations had occurred.

2.3. Protein expression and purification

The wild-type and mutant plasmids pET24d-KdcA-His were transformed into BL21(DE3)pLysS chemically competent cells (Promega). Cultures (1 L) were grown until $OD_{600} \approx 0.8$ and then induced with 1 mM IPTG. After overnight growth at room temperature, the cells were harvested, resuspended in buffer A (50 mM potassium phosphate buffer, pH 8.0, 500 mM NaCl, 10 mM imidazole), disrupted by sonication and cell debris removed by centrifugation. The cell free extract was applied to a Ni–NTA column connected to a BioLogic LP system (Bio-Rad) and eluted in buffer A containing 250 mM imidazole. The fractions of highest purity were pooled and the buffer was exchanged for storage buffer (100 mM potassium phosphate buffer, pH 6.0, 1 mM $MgSO_4$, 0.5 mM ThDP, and 10% glycerol) using Econo-Pac 10 DG desalting columns (Bio-Rad). The protein samples were concentrated with Amicon Ultra centrifugal filters (Millipore).

The WT enzyme and all KdcA variants were homogeneous as evaluated by SDS–PAGE. Protein concentrations were determined with the Bradford assay [18] using bovine serum albumin as standard.

2.4. Assay of decarboxylase activity

The decarboxylation of 2-keto acids was measured at 30 °C using a modified coupled enzymatic assay previously described for benzoylformate decarboxylase activity [7]. The assay mixture contained 0.2 mM NADH, 0.5 units/mL horse liver alcohol dehydrogenase and the 2-keto acid in assay buffer (50 mM potassium phosphate buffer, pH 6.0, 1 mM $MgSO_4$, 0.5 mM ThDP) in a total volume of 1 mL. The reaction was initiated by adding 0.5–100 μg of enzyme diluted in storage buffer, and the consumption of NADH was monitored at 340 nm with a Cary 50 Bio spectrophotometer (Varian).

One unit is defined as the amount of enzyme that catalyzes the decarboxylation of 1 μmol of 2-keto acid per minute at 30 °C under standard conditions.

2.5. Kinetic analysis

Initial velocity data were fitted to the Michaelis–Menten equation using the program Origin™ 5.0. Kinetic parameters were determined per monomer using a molecular mass of 60,884 Da. Additionally, data were fitted to the Hill equation, and in all cases $n_H \approx 1.0$.

3. Results and discussion

3.1. Expression and characterization of KdcA

When first reported, KdcA had been overexpressed in *L. lactis* and crude extracts were used to determine its pH optimum (ca. 6.0). In addition, its relative activity with a spectrum of potential substrates was measured by static headspace gas chromatography [11]. The results indicated that 3-methyl-2-oxobutanoic acid, the product of the catabolic transamination of valine, was the preferred substrate. 4-Methyl-2-oxopentanoic acid and 3-methyl-2-oxopentanoic acid, the products of leucine and isoleucine catabolism, respectively, were also readily accepted. Overall, the substrate spectrum of KdcA looked very similar to that of α-ketoisovalerate decarboxylase from *L. lactis*, with which it shares almost 90% sequence identity [19]. Of particular interest to us was the observation that 2-oxopentanoic acid and 2-oxohexanoic acid were also good substrates for KdcA. Previously, the latter had been shown to be the preferred substrate for the I472A variant of *Zm*PDC and both were also substrates for BFD A460I [10]. It was thought that comparing the three dimensional structures and the substrate specificities of *Zm*PDC, KdcA, IPDC, and BFD could provide insight into the evolution of substrate specificity across the ThDP-dependent decarboxylases.

Accordingly, the *kdcA* gene was cloned and KdcA expressed as its 6× His tagged variant (hereafter referred to as the wild-type (WT) enzyme) and was assayed with a variety of substrates (Table 1). In line with the earlier study, the highest k_{cat} values were observed with the branched chain 2-keto acids. However, the k_{cat} value for phenylpyruvate was about 60% that of the branched chain derivatives. The k_{cat} value decreased to about 6% of WT for the tyrosine catabolite, 4-hydroxyphenylpyruvate. In some respect there were more surprises in the K_m data than the k_{cat} data (Table 1). Broadly speaking, the aliphatic 2-keto acids had K_m values in the 1–3 mM range. By contrast, phenylpyruvate had a K_m value of 0.2 mM and, at 129 $mM^{-1}s^{-1}$, by far the highest value of k_{cat}/K_m. It is interesting to note that, although 4-hydroxyphenylpyruvate had the second lowest K_m value, its k_{cat} value was 10-fold lower than that of phenylpyruvate, suggesting that its binding was not

Table 1
Substrate specificity of KdcA[a]

Substrate	K_m (mM)	k_{cat} (s^{-1})	k_{cat}/K_m (mM^{-1} s^{-1})
Phenylpyruvic acid	0.21 ± 0.06	27 ± 3	129
3-Methyl-2-oxopentanoic acid	0.76 ± 0.05	41 ± 1	54
2-Oxohexanoic acid	0.60 ± 0.09	13 ± 1	21
3-Methyl-2-oxobutanoic acid	2.8 ± 0.3	48 ± 2	17
4-Methyl-2-oxopentanoic acid	3.7 ± 0.3	49 ± 2	13
2-Oxopentanoic acid	1.3 ± 0.2	9.9 ± 0.4	7.8
4-Hydroxyphenylpyruvic acid	0.63 ± 0.03	2.9 ± 0.1	4.6
4-Methylthio-2-oxobutanoic acid	2.4 ± 0.9	8.7 ± 1.3	3.6
Benzoylformic acid	7.5 ± 0.4	7.3 ± 0.2	0.97
Pyruvic acid	n.d.[b]	n.d.[b]	0.085[c]

[a] Results are the average ± standard deviation of three independent experiments.
[b] Not determined.
[c] Measured under V/K conditions (i.e., $[S] \ll K_m$).

optimal for catalysis. Overall, pyruvate and benzoylformate, the substrates of *Zm*PDC and BFD, respectively, had the lowest values of k_{cat}/K_m. While some activity was found with pyruvate, the levels were very low and saturation could not be reached even at substrate concentrations as high as 70 mM. Therefore k_{cat}/K_m, the value of the apparent second order rate constant for reaction with pyruvate, was determined from plots of reaction rate versus substrate concentration under conditions such that the pyruvate concentration was much lower than its K_m value. Conversely, the k_{cat} value for benzoylformate was in the range of the slower aliphatic substrates, but its value of K_m was the highest of those measured.

Many PDCs, including *Sc*PDC, display the sigmoidal kinetics indicative of substrate activation [20–22]. KdcA showed no evidence for substrate activation, and fitting kinetic data to the Hill equation provided n_H values ≈1.0 (data not shown). In this respect KdcA was similar to *Zm*PDC, IPDC and BFD all of which obey Michaelis–Menten kinetics [7,8,23].

3.2. Homology modeling

A homology model of KdcA was built based on the solved crystal structures of three other ThDP-dependent decarboxylases. KdcA shares 36%, 31%, and 41% sequence identity with *Zm*PDC, *Sc*PDC and IPDC, respectively. Modeling based on templates with >40% sequence identity is generally guaranteed to be successful, but in the case of lower identities, errors can be significantly reduced by employing an accurate sequence alignment [12,24,25]. In this case, the structure of IPDC was chosen as the initial template because it had the highest sequence identity with KdcA. The structure of *Zm*PDC was also included as a template because, despite its lower sequence identity with KdcA, it improved the quality of the model in some specific regions. In particular, *Zm*PDC was used to model the loop between residues 340–360, which aligns with a disordered area in the IPDC crystal structure (residues 342–355) (Fig. 2). Later the *Sc*PDC structure was also incorporated

```
KdcA    1   ---MYTVGDYLLDRLHELGIEEIFGVPGDYNLQFLDQIIS-REDMKWIGNANELNASYMADGYARTKK-AAAFLTTFGVGELSAINGLAGSYAENLPVVE
ZmPDC   1   --MSYTVGTYLAERLVQIGLKHHFAVAGDYNLVLLDNLLLN-KNMEQVYCCNELNCGFSAEGYARAKG-AAAAVVTYSVGALSAFDAIGGAYAENLPVIL
IPDC    1   MRTPYCVADYLLDRLTDCGADHLFGVPGDYNLQFLDHVID-SPDICWVGCANELNASYAADGYARCKG-FAALLTTFGVGELSAMNGIAGSYAEHVPVLH
BFD     1   ---MASVHGTTYELLRRQGIDTVFGNPGSNELPFLKDFP---EDFRYILALQEACVVGIADGYAQASRKPAFINLHSAAGTGNAMGALSNAWNSHSPLIV

KdcA   96   IVGSPTSKVQNDGKFVHHTLADGDFK--HFMKMHEPVTAARTLLTAENATYEIDRVLSQLLKERKPVYINLPVDVAAAKAEKPALSLEKESSTTN---TT
ZmPDC  97   ISGAPNNNDHAAGHVLHHALGKTDYH-YQLEMAKNITAAAEAIYTPEEAPAKIDHVIKTALREKKPVYLEIACNIASMPCAAPGPASALFNDEAS-DEAS
IPDC   99   IVGAPGTAAQQRGELLHHTLGDGEFR--HFYHMSEPITVAQAVLTEQNACYEIDRVLTTMLRERRPGYLMLPADVAKKAATPPVNALTHKQAHADS--AC
BFD    95   TAGQQ--TRAMIGVEALLTNVDAANLP-----RPLVKWSYEPASAAEVPHAMSRAIHMASMAPQGPVYLSVPYDDWDKDADPQSHHLFDRHVSSS--VRL

KdcA  191 EQVILSKIEESLKNAQKPVVIAGHEVISFGLEKTVTQFVSETKLPITTLNFGKSA-VDESLPSFLGIYNGKLSEISLKNFVESADFILMLGVKLTDSSTG
ZmPDC 195 LNAAVEETLKFIANRDKVAVLVGSKLRAAGAEEAAVKFADALGGAVATMAAAKSF-FPEENPHYIGTSWGEVSYPGVEKTMKEADAVIALAPVFNDYSTT
IPDC  195 LKAFRDAAENKLAMSKRTALLADFLVLRHGLKHALQKWVKEVPMAHATMLMGKGI-FDERQAGFYGTYSGSASTGAVKEAIEGADTVLCVGTRFTDTLTA
BFD   186 NDQDLDILVKALNSASNPAIVLGPDVDAANANADCVMLAERLKAPVWVAPSAPRCPFPTRHPCFRGLMP--AGIAAISQLLEGHDVVLVIGAPVFRYHQY

KdcA  290 AFTHHLDE-NKMISLNIDEGIIFNKVVEDFDFRAVVSSLSELKGIEYEG--QYIDKQYEEFI-----PSSAPLSQDRLWQAVESLTQSNETIVAEQGTSF
ZmPDC 294 GWTDIPDP-KKLVLAEPRSVVVNGIRFPSVHLKDYLTRLAQKVSKKTGALDFFKSLNAGELKKAAPADPSAPLVNAEIARQVEALLTPNTTVIAETGDSW
IPDC  294 GFTHQLTP-AQTIEVQPHAARVGDVWFTGIPMNQAIETLVELCKQHVHAGLMSSSSGAIPFP-----QPDGSLTQENFWRTLQTFIRPGDIILADQGTSA
BFD   284 DPGQYLKPGTRLISVTCDPLEAARAPMGDAIVADIGAMASALANLVEESSRQLPTAAPEPAK---VDQDAGRLHPETVFDTLNDMAPENAIYLNESTSTT

KdcA  382 FGASTIFLKSNSRFIGQPLWGSIGYTFPAALGSQIADKESRHLLFIGDGSLQLTVQELGLSIREKLNPICFIINNDGYTVEREIHGPTQSYNDIPMWNYS
ZmPDC 393 FNAQRMKLPNGARVEYEMQWGHIGWSVPAAFGYAVGAPERRNILMVGDGSFQLTAQEVAQMVRLKLPVIIFLINNYGYTIEVMIH--DGPYNNIKNWDYA
IPDC  388 FGAIDLRLPADVNFIVQPLWGSIGYTLAAAFGAQTACPNRRVIVLIGDGAAQLTIQELGSMLRDKQHPIILVLNNEGYTVERAIHGAEQRYNDIALWNWT
BFD   381 AQMWQRLNMRNPGSYYFCAAGQLGFALPAAIGVQLAEPERQVIAVIGDGSANYSISALWTAAQYNIPTIFVIMNNGTYGALRWFAGVLEAENVPGLDVPG

KdcA  482 KLPETFGATEDRVVSKIVRTENEFVSVMKEAQADVNR----MYWIELVLEKEDAPKLLKKMGKLFAEQNK--------
ZmPDC 491 GLMEVFNGNGGYDSGAGKGLKAKTGGELAEAIKVALANTDGPTLIECFIGREDCTEELVKWGKRVAAANSRKPVNKLL
IPDC  488 HIPQALSLDPQSECWRVS--EAEQLADVLEKVAHHER----LSLIEVMLPKADIPPLLGALTKALEACNNA--------
BFD   481 IDFRALAKGYGVQALKADNLEQLKGSLQEALS------AKGPVLIEVSTVSPVK----------------------
```

Fig. 2. Alignment of ThDP-dependent 2-keto acid decarboxylases. The residues studied in this work are indicated by black triangles. The boxes designate residues involved in catalysis and cofactor binding. The disordered region in the IPDC structure is indicated by a gray line.

in the building of the model because, unlike the structures of IPDC and *Zm*PDC, it has an inhibitor (pyruvamide) bound in the active site in addition to ThDP.

Using Modeller 8v2, after iterative manual refinements of the alignment to accommodate insertions and deletions of the query sequence respect to the templates in the optimal manner, 32 models of the monomer were generated. Verify_3D and PROCHECK were used to evaluate the models, and to identify the one with the best structural compatibility. The final model of KdcA, which was used in structural analysis, is dimeric and includes both ThDP and pyruvamide.

The model of the monomer (Fig. 3A) is compatible with the α/β topology observed in all ThDP-dependent decarboxylases crystallized to date [26]. Each monomer comprises the N-terminal (Pyr) domain, a middle domain and the C-terminal (PP) domain. Two monomers are required to form the active site, which includes contributions from the Pyr and PP domains of each monomer. These bind the pyrimidine ring and the diphosphate tail of ThDP, respectively [26]. The region of the active site comprises the ThDP binding motif (Fig. 2), the catalytic glutamic acid residue (Glu49) and the hydrophobic residue (Ile404) which holds the cofactor in its typical "V"-conformation. There is also a pair of catalytic histidine residues. This pair is formed by two contiguous histidines in IPDC and the PDCs, but in BFD the two histidines come from loops in two different monomers. In KdcA, the two histidines are contiguous (Fig. 3B) suggesting that KdcA has evolved from a PDC-like precursor. Conceivably, it should be possible to alter the binding site of KdcA sufficiently for it to accept pyruvate as a reasonable substrate.

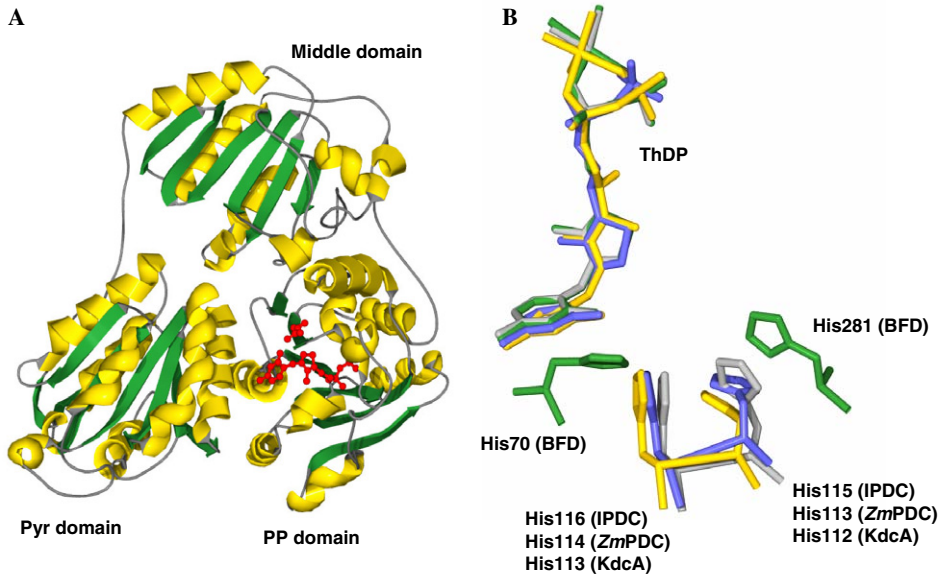

Fig. 3. Structural model of *Lactococcus lactis* KdcA. (A) Cartoon representation of the monomer highlighting the three domain structure. The molecules of ThDP and pyruvamide are included as ball-and-stick models. (B) Superimposition of active site histidines from BFD (green), *Zm*PDC (gold), IPDC (blue) and KdcA (gray). The figure was obtained using the coordinates from 1BFD, 1ZPD, 1OVM and the homology model of KdcA. (For interpretation of the references to colour in this figure legend, the reader is referred to the web version of this article.)

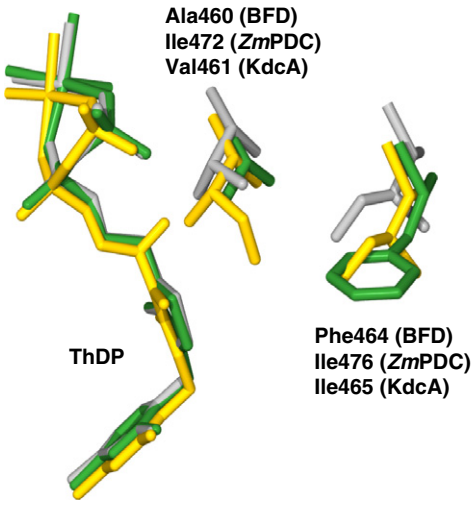

Fig. 4. Putative substrate binding residues of *Zm*PDC (green), BFD (gold), and KdcA (gray). The corresponding residues in *Zm*PDC and BFD were previously studied by site-directed mutagenesis [10]. (For interpretation of the references to colour in this figure legend, the reader is referred to the web version of this article.)

According to this model, Val461 in KdcA is structurally equivalent to Ala460 in BFD and Ile472 in *Zm*PDC (Fig. 4). This position has been studied in the two latter enzymes, and it has been shown that swapping this residue generates PDC and BFD enzymatic variants with increased ability to decarboxylate branched chain 2-keto acids [10]. Therefore, reverse engineering would suggest that the V461I mutation should result in an increase in affinity for pyruvate.

The fact that *Zm*PDC has a much more limited substrate spectrum than *Sc*PDC is well established [27]. In the former, the bulky aromatic residues, Tyr290, Trp392, and Trp551, are thought to restrict the size of the binding pocket and thereby prevent the binding of larger substrates [2]. In a multiple alignment of plant and bacterial PDCs aromatic side chains in the equivalent positions are conserved (data not shown). The exceptions are the yeast PDCs which have smaller residues in those positions. In *Sc*PDC, for example, Trp392 is replaced by alanine and, when the W392A variant of ZmPDC was prepared, it was found to have an expanded range of activity [27,28]. In the IPDC structure the corresponding residues are Thr290, Ala387, and Leu542. *In toto* these substitutions account for the difference in volume of the active site cavity observed between the *Zm*PDC and IPDC structures (130 $Å^3$ in IPDC compared to 85 $Å^3$ in *Zm*PDC, [5]). The structural homologues in the KdcA model are Ser286, Phe381, and Met538 (Fig. 5). Each of these residues is smaller than its *Zm*PDC counterpart and it was thought that conversion of the individual residues, in turn, to its *Zm*PDC analogue, would decrease the volume of the active site cavity of KdcA and may provide a variant with increased pyruvate decarboxylase activity.

3.3. Site-directed mutagenesis

The KdcA variants, V461I, S286Y, F381W and M538W, were constructed, expressed and purified to apparent homogeneity as described under Section 2. During purification

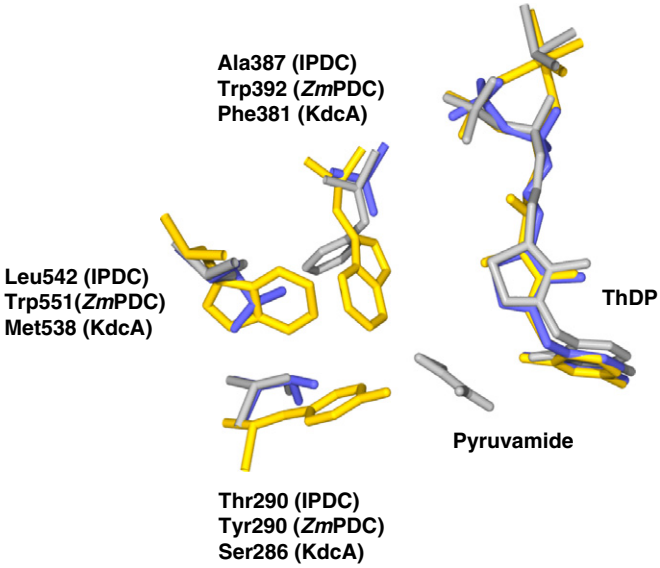

Fig. 5. Residues in the putative substrate binding pocket of *Zm*PDC (gold), lPDC (blue), and KdcA (gray). The molecule of pyruvamide is an indicator of the putative position of the KdcA substrate. (For interpretation of the references to colour in this figure legend, the reader is referred to the web version of this article.)

the four mutant enzymes showed physical properties essentially identical to those of WT KdcA. However, all of the variants showed an increase in their ability to decarboxylate pyruvate (Table 2).

Pyruvate is not a good substrate for WT KdcA and, while there is evidence for decarboxylase activity, the enzyme is not saturated even at high pyruvate concentrations. By contrast all the mutants showed saturation kinetics, with K_m values between 20–65 mM. Perhaps more impressive was the increase in k_{cat} values, particularly for the S286Y and F381W variants which had values of 17 s^{-1} and 26 s^{-1}, respectively. To put this into context, the k_{cat} value for WT KdcA with phenylpyruvate, its optimum substrate based on k_{cat}/K_m values, was 27 s^{-1}. The results show clearly that, while there is room for an improvement in binding affinity for pyruvate, the trend is in the right direction.

Presumably, if the KdcA substrate binding site has been made smaller, this should be reflected in decreased affinity for the larger substrates. The results in Table 2, in general confirm this hypothesis. This was particularly evident for the S286Y variant which exhibited a relatively low K_m value for pyruvate but showed 25- and 30-fold increases in K_m values for 3-methyl-2-oxopentanoic acid and phenylpyruvate, respectively. There were also some anomalies: the M538W variant, for example, had the lowest K_m value for pyruvate. It also showed 6-fold increases in K_m values for 3-methyl-2-oxopentanoic acid and benzoylformate, yet had a lower K_m value for phenylpyruvate than that of WT KdcA. The F381W variant was also surprising, in that it had the highest k_{cat} value for pyruvate but, essentially, an unchanged value for phenylpyruvate. It also showed a 4.5-fold increase in k_{cat} for 3-methyl-2-oxopentanoic acid. The reasons for the anomalous results remain unclear.

Table 2
Kinetic constants for decarboxylase activity of KdcA variants[a,b]

KdcA variant	3-Methyl-2-oxopentanoic acid			Pyruvic acid			Benzoylformic acid			Phenylpyruvic acid		
	k_{cat} (s^{-1})	K_m (mM)	k_{cat}/K_m ($mM^{-1}\ s^{-1}$)	k_{cat} (s^{-1})	K_m (mM)	k_{cat}/K_m ($mM^{-1}\ s^{-1}$)	k_{cat} (s^{-1})	K_m (mM)	k_{cat}/K_m ($mM^{-1}\ s^{-1}$)	k_{cat} (s^{-1})	K_m (mM)	k_{cat}/K_m ($mM^{-1}s^{-1}$)
WT	40	0.76	53	ND	ND	0.085	7.3	7.5	1.0	27	0.21	128
V461I	14	1.1	13	2.3	18	0.13	3.1	2.2	1.4	2.9	2.3	1.3
S286Y	35	19	1.8	17	34	0.5	2.1	6.9	0.3	2.5	6.3	0.4
F381W	177	1.7	104	26	65	0.4	9.4	6.2	1.5	20	0.17	117
M538W	12	5.5	2	2.5	22	0.11	4.7	46	0.1	0.7	0.1	7.0

[a] Reactions were carried out at 30 °C as described under Experimental Procedures.
[b] Errors are estimated to be ±10% from triplicate measurements.

Overall, the mutagenesis results confirmed predictions based on the KdcA homology model, i.e., that Val461, Ser286, Phe381, and Met538 each contributes to substrate binding and catalysis by KdcA. However, the results also showed that mutation of a single residue was unlikely to provide an "instant" conversion to KdcA into a PDC. Therefore, in preliminary experiments, combinations of double mutants as well as the triple mutant were generated for the S286Y, F381W, and M538W variants. Unfortunately, these mutant enzymes had impaired solubility and stability, and preliminary experiments suggest that they have extremely low activity towards the substrates tested in this work (data not shown). We have now turned our attention towards saturation mutagenesis to identify candidates with improved PDC activity.

Acknowledgments

This paper is dedicated to the memory of Miriam S. Hasson, a collaborator and friend, whose presence is sorely missed. The work was supported by a Frontiers in Integrative Biology Research Grant (EF 0425719) from the National Science Foundation (M.J.M. and G.L.K.).

Appendix A. Supplementary data

Supplementary data associated with this article can be found, in the online version, at doi:10.1016/j.bioorg.2006.08.005.

References

[1] A. Schellenberger, Biochim. Biophys. Acta 1385 (1998) 177–186.
[2] D. Dobritzsch, S. Konig, G. Schneider, G. Lu, J. Biol. Chem. 273 (1998) 20196–20204.
[3] P. Arjunan, T. Umland, F. Dyda, S. Swaminathan, W. Furey, M. Sax, B. Farrenkopf, Y. Gao, D. Zhang, F. Jordan, J. Mol. Biol. 256 (1996) 590–600.
[4] M.S. Hasson, A. Muscate, M.J. McLeish, L.S. Polovnikova, J.A. Gerlt, G.L. Kenyon, G.A. Petsko, D. Ringe, Biochemistry 37 (1998) 9918–9930.
[5] A. Schütz, T. Sandalova, S. Ricagno, G. Hübner, S. König, G. Schneider, Eur. J. Biochem. 270 (2003) 2312–2321.
[6] M. Pohl, P. Siegert, K. Mesch, H. Bruhn, J. Grotzinger, Eur. J. Biochem. 257 (1998) 538–546.
[7] P.M. Weiss, G.A. Garcia, G.L. Kenyon, W.W. Cleland, P.F. Cook, Biochemistry 27 (1988) 2197–2205.
[8] A. Schütz, R. Golbik, K. Tittmann, D.I. Svergun, M.H. Koch, G. Hübner, S. König, Eur. J. Biochem. 270 (2003) 2322–2331.
[9] M.J. McLeish, G.L. Kenyon, E.S. Polovnikova, A.S. Bera, N.L. Anderson, M.S. Hasson, in: F. Jordan, M.S. Patel (Eds.), Catalytic mechanisms and role in normal and disease states, Marcel Dekker Inc., New York, 2004, pp. 131–141.
[10] P. Siegert, M.J. McLeish, M. Baumann, M.M. Kneen, G.L. Kenyon, M. Pohl, Prot. Eng. Des. Sel. 18 (2005) 345–357.
[11] B.A. Smit, J.E.T. van Hylckama Vlieg, W.J.M. Engels, L. Meijer, J.T.M. Wouters, G. Smit, Appl. Environ. Microbiol. 71 (2005) 303–311.
[12] R. Sanchez, A. Sali, in: D.M. Webster (Ed.), Protein structure prediction, methods and protocols, Humana Press, New Jersey, 2000, pp. 97–129.
[13] D. Higgins, J. Thompson, T. Gibson, J.D. Thompson, D.G. Higgins, T.J. Gibson, Nucleic Acids Res. 22 (1994) 4673–4680.
[14] L.J. McGuffin, K. Bryson, D.T. Jones, Bioinformatics 16 (2000) 404–405.
[15] R. Luthy, J.U. Bowie, D. Eisenberg, Nature 356 (1992) 83–85.
[16] R.A. Laskowski, M.W. MacArthur, D.S. Moss, J.M. Thornton, J. Appl. Crystallogr. 26 (1993) 283–291.

[17] N. Guex, M.C. Peitsch, Electrophoresis. 18 (1997) 2714–2723.
[18] M.M. Bradford, Anal. Biochem. 72 (1976) 248–254.
[19] M. de la Plaza, P. Fernandez de Palencia, C. Pelaez, T. Requena, FEMS Microbiol. Lett. 238 (2004) 367–374.
[20] G. Hübner, R. Weidhase, A. Schellenberger, Eur. J. Biochem. 92 (1978) 175–181.
[21] F. Krieger, M. Spinka, R. Golbik, G. Hübner, S. König, Eur. J. Biochem. 269 (2002) 3256–3563.
[22] Q. Wang, P. He, D. Lu, A. Shen, N. Jiang, J. Biochem. (Tokyo) 136 (2004) 447–455.
[23] S. Bringer-Meyer, K.L. Schimz, H. Sahm, Arch. Microbiol. 146 (1986) 105–110.
[24] R. Sanchez, A. Sali, Curr. Opin. Struc. Biol. 7 (1997) 206–214.
[25] A. Tramontano, Methods 14 (1998) 293–300.
[26] R. Duggleby, Acc. Chem. Res. in press.
[27] H. Iding, P. Siegert, K. Mesch, M. Pohl, Biochim. Biophys. Acta 1385 (1998) 307–322.
[28] H. Bruhn, M. Pohl, J. Grötzinger, M.-R. Kula, Eur. J. Biochem. 234 (1995) 650–655.